Available online at www.sciencedirect.com
SCIENCE DIRECT®
International Journal of Solids and Structures 43 (2006) 3626–3642
INTERNATIONAL JOURNAL OF SOLIDS and STRUCTURES
www.elsevier.com/locate/ijsolstr

Application of BEM and optimization technique to wear problems

G.K. Sfantos, M.H. Aliabadi *

Department of Aeronautics, Faculty of Engineering, Imperial College, University of London, South Kensington Campus, Prince Consort Road, London SW7 2BY, UK

Received 3 March 2005; received in revised form 1 June 2005
Available online 2 November 2005

Abstract

In this paper a new method for solving wear problems, using the Boundary Element Method (BEM) is proposed. The proposed method uses a shape optimization technique for rapid calculation of the maximum wear depth and the final geometry of the bodies in contact after a specified service period. The optimization method solves the wear problem directly, without using increments of the sliding distance as in the classical methods. The BEM is used for modelling both bodies in contact, treating the problem as a multi-region problem. The material loss is presented in terms of the applied load and the sliding distance, and is modelled using a linear wear model. The proposed method is shown to be robust as it requires only few iterations to achieve a converged solution. The reduction in computational effort, as compared to the classical incremental method, becomes more significant as the sliding distance increases.

Keywords: Wear; Boundary element method; Contact analysis; Optimization

1. Introduction

Machine maintenance is receiving more attention nowadays, as it is directly linked to a reduction in the operational cost. Traditionally the maintenance of a machine was basically the replacement of a component when and if a problem occurred. However as this process is expensive, not only due to repair of machines but also because of the interruption to the production line, new methods have been developed to minimize the total cost. Machine maintenance is required as components are worn in service. Therefore in order to schedule the optimum periods for replacement of machine components, wear predictions should be carried out; hence maintenance periods could be scheduled a priori, and the design of a mechanical component could be optimized in terms of reducing the wear.

* Corresponding author. Tel.: +44 20 7594 5077; fax: +44 20 7594 5078.
E-mail address: m.h.aliabadi@imperial.ac.uk (M.H. Aliabadi).

0020-7683/$ - see front matter
doi:10.1016/j.ijsolstr.2005.09.004

For simulating a wear problem, the sliding contact problem of one body over another body, must be solved first, as the phenomenon of wear is closely related to the resulting pressure distribution inside the contact area. Knowing the contact pressure distribution, the *wear depth* can be evaluated using a *wear model*. The wear model that describes a specific problem varies with respect to the *wear mechanism* (Lim and Ashby, 1987). The commonly used wear model is due to Archard (1953) and is known as the linear model for delamination wear, where the volume of wear is proportional to the normal load. Thus for a specific sliding distance the volume of material loss can be calculated if the normal load and the wear coefficient (that includes material properties, friction, etc.) are known. These models can be calibrated from experiments for specific pair of materials so that the wear coefficients are evaluated.

Due to the complex configuration of most mechanical components, a numerical method is used to solve the contact problem, particularly in cases where the contacted geometries do not obey the Hertzian assumptions (Hertz, 1882). The main difficulty is due to changes in contact area with respect to time as one or both bodies lose material. Hence the pressure distribution changes as a function of the topography of the potential contact area and the sliding distance, machining time, etc. In reality the function of the pressure distribution with respect to the sliding distance and the contact topography is unknown. Thus, to simulate a wear problem, the total sliding distance is divided into small increments and the whole problem is solved for each sliding increment, updating every time the geometries of the bodies. For each small sliding increment the contact problem is solved and the pressure distribution inside the contact area is determined. Next using a wear model the wear depth is evaluated and the geometry of the worn body is updated. This method is the classic *Incremental Method* that is commonly used for wear simulation problems (Põdra and Andersson, 1999a,b), for simulating a machining process (MacGinley and Monaghan, 2001; Yen et al., 2004) and for simulating wear in bioengineering as in total hip and knee prosthesis (Maxian et al., 1996a,b; Wu et al., 2003). The convergence is achieved as the sliding increment decreases.

The application of the Finite Element Method (FEM) to modelling wear is well established (Põdra and Andersson, 1999a,b; MacGinley and Monaghan, 2001; Yen et al., 2004; Maxian et al., 1996a,b; Wu et al., 2003). The main reason is that the FEM are widely available and it's relatively easy nowadays to use a commercial FEM package. On the other hand, the application of the Boundary Element Method (BEM) to wear problems is relatively new. An application of BEM to modelling wear has been reported by Serre et al. (2001). The problem modelled was a cross section of a ring on a ring, resulting in a conformal contact. The case in which only one body could be worn was considered. Recently Sfantos and Aliabadi (in press) presented a boundary element formulation for multi-body wear simulation using an incremental method.

An alternative method for finding the asymptotic state of a wear problem, by solving a minimization problem, has been recently reported by Peigney (2004). The problem modelled was a cyclically moving rigid indenter over a half plane, and the main objective was to estimate the asymptotic wear state by minimizing the energy dissipated in the wear process. In the present work a new method is presented that solves directly the wear problem, without using increments of the sliding distance, for a specified service period. It will be referred to as the *Optimization Method* as it uses a first order optimization technique to solve the wear problem, in terms of *Shape Optimization* (Mellings and Aliabadi, 1995; Aliabadi and Mellings, 1997; Martinez et al., 1998). The main advantage of the proposed method is the considerable reduction in computational effort compared to the traditional *Incremental Method*.

2. Wear model

The *Wear Rate* of a body sliding over another body is a dynamic phenomenon as it changes with respect to the time. Even if the external conditions (applied force, sliding velocity, etc.) were constant, the properties, the condition and the geometry of the contact surfaces are changing, thus resulting in the variation of the wear rate.

Conventionally wear rate $\dot{W}$ is defined as the volume loss W from the bearing surface per unit of sliding distance:

$$\dot{W} = \frac{\mathrm{d}W}{\mathrm{d}S} \tag{1}$$

The wear rate $\dot{W}$ is a function of the applied load (P), the relative velocity of the two contacting surfaces (v), their initial temperatures (T) and the properties of the materials that come into contact. Therefore the wear rate may be described in a general form as

$$\dot{W} = f\{P, v, T, \text{material properties}\} \tag{2}$$

In the case where the sliding speed remains at low levels and the applied load does not exceed a limit where seizure takes place, the wear that occurs is characterized as *Delamination Wear*, which arises from the adhesive forces set up whenever atoms come into intimate contact (Rabinowicz, 1995). In delamination wear the sliding speed is low enough so that surface heating can be neglected. The model that describes this mechanism is the well known Archard's linear wear law (Archard, 1953), originally proposed by Holm (1946), given as

$$W^H = K^H \frac{P}{H_0} S \tag{3}$$

where W^H is the volumetric wear, for each body $H = \{A, B\}$ and K^H is the non-dimensional wear coefficient, that is dependent on the materials in contact and their exact degree of cleanliness (Rabinowicz, 1995). For every pair of materials that slide over each other, a specific constant K^H can be determined experimentally. H_0 denotes the hardness of the "softer" material in contact, which is being worn out. Eq. (3) describes the volume of material loss after S sliding distance, as long as the temperature increase is negligible.

In order to simulate wear using a computational technique, a wear model must be used. Using a wear model the parameter "*sliding material*" is introduced in the formulation. Consequently the wear model and its calibration is irreplaceable. However the model described by Eq. (3) does not provide sufficient details. For that reason instead of the wear volume the *Wear Depth* can be used for simulating the worn geometry as the sliding goes on. Moreover the wear depth is of great practical importance in every day engineering as it can be measured directly on a specific mechanical component.

In the two-dimensional case, as Fig. 1 illustrates, the above model describes the volume of material loss per unit thickness, with respect to the sliding distance S, when a specific load P per unit thickness is applied. Taking the first derivative of Eq. (3) with respect to the width of the contact area, the wear depth is given as

$$h^H(\mathbf{x}, s) = k^H p(\mathbf{x}, s) s \tag{4}$$

where $h^H(\mathbf{x}, s)$ is the corresponding wear depth of a point $\mathbf{x}$ on the bearing surface of each body $H = \{A, B\}$, that has travelled s sliding distance, $p(\mathbf{x}, s)$ is the pressure distribution developed inside the contact area and k^H is the modified Archard's wear coefficient given by $k^H = K^H/H_0$. Both pressure and wear depth are functions of the location and the sliding distance as the bodies lose material during the wear process and the topography of their bearing surfaces changes. Furthermore, in cases as a pin on a rotating disc problem, the travelled distance s by each point $\mathbf{x}$ on the bearing surfaces is also a function of the location of the point. However this sliding distribution with respect to the location of each point on the bearing surfaces can be evaluated directly

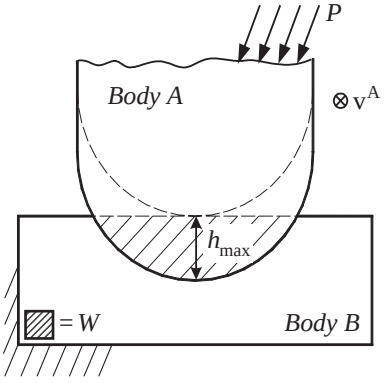

Fig. 1. Schematic representation of wear. Body B wears out due to the sliding of body A (v^A is normal to Figure's plane). The volumetric wear W and the maximum wear depth h_{max} are illustrated.

by the kinematics of the specific tribosystem. The direction of wear, the wear vector, is taken to coincide with the pressure vector; that is normal to the bearing surface of the body in contact.

3. Contact mechanics

The formulation used for modelling two solids in contact is similar to the *Multi-Region* formulation (Aliabadi, 2002). The main feature is the displacements and tractions inside the contact area remain unknown. Here only the basics will be outlined. For a more detailed review the authors are referred to Man et al. (1993a,b) and Aliabadi (2002).

The potential contact boundary is denoted as S_{c}^{H} and the non-contact boundary as S_{nc}^{H}, as Fig. 2 illustrates.

$$S^{H} = S_{\mathrm{nc}}^{H} \cup S_{\mathrm{c}}^{H}, \quad H = \{A, B\} \tag{5}$$

The displacement integral equation (Aliabadi, 2002) for the bodies shown in Fig. 2, can be written as

$$C_{ij}^{H}(\mathbf{x}')u_{j}^{H}(\mathbf{x}') + \oint_{S_{\mathrm{nc}}^{H}} T_{ij}^{H}(\mathbf{x}', \mathbf{x})u_{j}^{H}(\mathbf{x})\,\mathrm{d}S_{\mathrm{nc}}^{H} + \oint_{S_{\mathrm{c}}^{H}} T_{ij}^{H}(\mathbf{x}', \mathbf{x})u_{j}^{H}(\mathbf{x})\,\mathrm{d}S_{\mathrm{c}}^{H}$$
$$= \int_{S_{\mathrm{nc}}^{H}} U_{ij}^{H}(\mathbf{x}', \mathbf{x})t_{j}^{H}(\mathbf{x})\,\mathrm{d}S_{\mathrm{nc}}^{H} + \int_{S_{\mathrm{c}}^{H}} U_{ij}^{H}(\mathbf{x}', \mathbf{x})t_{j}^{H}(\mathbf{x})\,\mathrm{d}S_{\mathrm{c}}^{H} \tag{6}$$

where u_{j}^{H}, t_{j}^{H} are components of displacements and tractions, respectively, for each body $H = \{A, B\}$, $U_{ij}^{H}(\mathbf{x}', \mathbf{x})$, $T_{ij}^{H}(\mathbf{x}', \mathbf{x})$ are the fundamental solution representing the displacements and the tractions, respectively, in the j direction at a point $\mathbf{x}$ due to a unit point force in the i direction at point $\mathbf{x}'$ and C_{ij}^{H} is the so-called "free term" (Aliabadi, 2002).

To solve the boundary integral equation (6) the boundaries S_{c}^{H} and S_{nc}^{H} of each body $H = \{A, B\}$ are discretized into N_{c}^{H} and N_{nc}^{H} elements respectively. Each element is composed of m_{c}^{H} and m_{nc}^{H} number of nodes for the contact and the non-contact elements, respectively. According to the *Multi-Region* technique (Aliabadi, 2002), the individual systems of equations are combined and the interface boundary conditions are subsequently applied. Considering both bodies in contact, body A and body B and after rearranging and applying the boundary conditions, the overall system of equations takes the following form:

$$\begin{bmatrix} \mathbf{A}_{\mathrm{nc}}^{A} & [0] & \overline{\mathbf{H}}_{\mathrm{c}}^{A} & [0] & -\overline{\mathbf{G}}_{\mathrm{c}}^{A} & [0] \\ [0] & \mathbf{A}_{\mathrm{nc}}^{B} & [0] & \overline{\mathbf{H}}_{\mathrm{c}}^{B} & [0] & -\overline{\mathbf{G}}_{\mathrm{c}}^{B} \\ [0] & [0] & [& & \mathbf{BC}_1 &] \\ [0] & [0] & [0] & [0] & [\quad \mathbf{BC}_2 &] \end{bmatrix} \begin{Bmatrix} \mathbf{x}_{\mathrm{nc}}^{A} \\ \mathbf{x}_{\mathrm{nc}}^{B} \\ \overline{\mathbf{u}}_{\mathrm{c}}^{A} \\ \overline{\mathbf{u}}_{\mathrm{c}}^{B} \\ \overline{\mathbf{t}}_{\mathrm{c}}^{A} \\ \overline{\mathbf{t}}_{\mathrm{c}}^{B} \end{Bmatrix} = \begin{Bmatrix} \mathbf{R}_{\mathrm{nc}}^{A} \cdot \mathbf{y}_{\mathrm{nc}}^{A} \\ \mathbf{R}_{\mathrm{nc}}^{B} \cdot \mathbf{y}_{\mathrm{nc}}^{B} \\ \mathbf{F}_1 \\ \mathbf{F}_2 \end{Bmatrix} \tag{7}$$

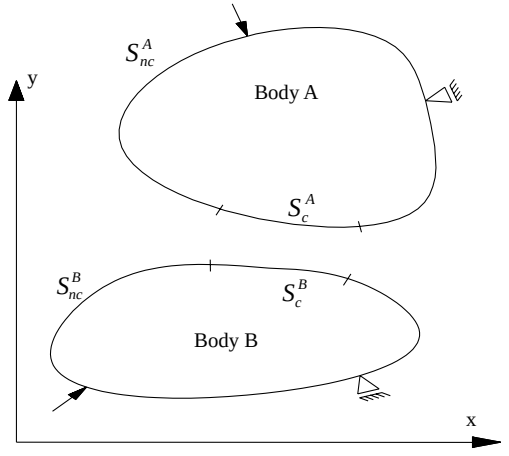

Fig. 2. The boundary division to contact and non-contact region.

Table 1
Boundary constraints

Separation	Contact—slip
$(t_c^A)_t - (t_c^B)_t = 0$	$(t_c^A)_t - (t_c^B)_t = 0$
$(t_c^A)_n - (t_c^B)_n = 0$	$(t_c^A)_n - (t_c^B)_n = 0$
$(t_c^A)_t = 0$	$(t_c^A)_t = 0$
$(t_c^A)_n = 0$	$(u_c^A)_n + (u_c^B)_n = \text{gap}^{A-B}$

Table 2
Contact mode check criteria

Assumption … Decision	Separation	Contact
Separation	$(u_c^A)_n + (u_c^B)_n < \text{gap}^{A-B}$	$(u_c^A)_n + (u_c^B)_n \geqslant \text{gap}^{A-B}$
Contact	$(t_c^{A \text{ or } B})_n \geqslant 0$	$(t_c^{A \text{ or } B})_n < 0$

where the matrices $\mathbf{A}_{nc}^H$ and $\mathbf{R}_{nc}^H$ are of size $2M^H X 2(M^H - M_c)$, for two dimensional bodies, containing known integrals of the product of the shape functions, the Jacobians and the fundamental fields T_{ij}^H and U_{ij}^H, after the substitution of the boundary conditions of the non-contact area of both bodies. The matrices $\overline{\mathbf{H}}_c^H$ and $\overline{\mathbf{G}}_c^H$ are of size $2M^H X 2M_c$, in local coordinates, and both contain known integrals of the product of the shape functions, the Jacobians and the fundamental fields T_{ij}^H and U_{ij}^H, respectively, corresponding to the potential contact nodes. The column vectors $\mathbf{x}_{nc}^H$ and $\mathbf{y}_{nc}^H$ have $2(M^H - M_c)$ components, containing the unknown and the known, respectively, components of tractions and displacements of the non-contact boundary, while the vectors $\overline{\mathbf{u}}_c^H$ and $\overline{\mathbf{t}}_c^H$ have $2M_c$ components each and contain the unknown boundary values of the potential contact area (in terms of displacements and tractions, respectively). M^H is the total number of nodes for each body $H = \{A, B\}$, and M_c is the total number of nodes of the potential contact-worn area of each body which is defined to be the same for both bodies.

The submatrix $\mathbf{BC}_1$ in Eq. (7) has $2M_c X 8M_c$ components and contains all the boundary conditions for the normal displacements and the tangential tractions for the contact node pairs, presented in Table 1 (Johnson, 2001) and also the constraints for the zero tangential and normal tractions for the pairs in separation mode. The submatrix $\mathbf{BC}_2$ has $2M_c X 4M_c$ components and contains all the boundary conditions for the equilibrium of the normal and tangential tractions. The column matrices $\mathbf{F}_1$ and $\mathbf{F}_2$ have $2M_c$ components each and contain the right-hand sides of the boundary conditions implemented in matrices $\mathbf{BC}_1$ and $\mathbf{BC}_2$. In order to obtain the correct contact area without any geometrical incompatibility and contact mode violations, the displacements and tractions for every node in the contact zone must be checked against the criteria presented in Table 2. The term gap^{A-B} in Tables 1 and 2 denotes the initial normal gap between the undeformed bodies (Aliabadi, 2002). A detailed review about the arrangement of these matrices can be found in Sfantos and Aliabadi (in press).

In the present work the contact problem is treated as frictionless. Considering a sliding wear non-conformal problem, where one body slides over another, the contact modes of the contact node pairs are *Slip* or *Separation* only.

The contact analysis starts with an initial guess of the contact node pairs. The coupled contact problem is solved and checks for any contact mode violations are made. If the initial guess for the contact node pairs that come into contact, for the specific applied normal load, was false, the assumed pairs are updated and the problem is solved again until no contact mode violations occur.

4. Optimization method

Optimization Methods can be used to provide a rapid solution to the wear problem, without using increments of the sliding distance. A wear Optimization Technique can be formulated in a similar way to *Shape Optimization* and *Shape Identification* problems (Mellings and Aliabadi, 1995; Aliabadi and Mellings, 1997; Martinez et al., 1998). The basic idea of the method is that a wear problem can be solved inversely. To reach

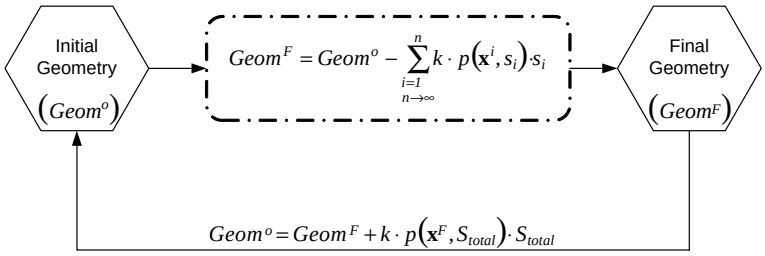

Fig. 3. Schematic presentation of a wear simulation procedure, (k = wear coefficient, $p(\mathbf{x}^i, s_i)$ = pressure distributions as a function of the contact area $\mathbf{x}^i$ after s_i sliding distances, where $\sum_{i=1}^{n} s_i = S_{\text{total}}$).

the final geometry from the initial geometry is a distance-time dependent problem, as the bodies lose material and the topography of their bearing surface changes altering the pressure distribution. However, in the inverse case of "knowing" the actual final geometry, and consequently the pressure distribution at that time, the procedure to determine the initial geometry, solving inversely, is not distance-time dependent,[1] as Fig. 3 illustrates. If the pressure distribution $p(\mathbf{x}, s)$, that is a function of the topography $\mathbf{x}$ and the sliding distance s, can be calculated for an assumed final geometry, which was produced after S_{total} sliding distance, the initial geometry can be determined directly through the modified wear law, Eq. (4), that describes the wear mechanism. The existence of the uniqueness of the solution states to the mechanical equilibrium of the system. Since the integral of any pressure distribution inside the contact area must always be equal to the applied load, the wear volume that is calculated by the wear model is always the same for every assumed final geometry (due to the fact that the wear volume is correlated with the applied load Eq. (3) for a given tribosystem). Consequently there will be only one final geometry, the actual one, that adding the material loss (wear distribution), calculated by the pressure distribution at that time using the modified wear law, Eq. (4), the initial geometry would be reached. Hence the problem now is stated as: find the final geometry, by assuming different geometries, and using the modified wear law for the developed pressure distribution of those geometries, the initial geometry could be calculated by adding on the assumed final geometry the evaluated wear depth distribution.

5. Wear depth function

In *Shape Optimization* and *Identification* (Mellings and Aliabadi, 1995; Aliabadi and Mellings, 1997; Martinez et al., 1998; Aliabadi, 2002) the design variables are usually nodal coordinates, that either are separate, corresponding to every single node, or are combined in a specific function that is used to update the geometry of a specific part of the body in consideration. In the wear *Optimization Method*, the design variables could be all the normal gaps of the discretized potential contact area of both bodies. Two main problems appear using the above mentioned scheme. Firstly it results in a large number of design variables, and secondly oscillations will occur when calculating the derivatives of the objective function.

On the other hand considering a realistic wear experiment, e.g. a pin on a rotating disc, the way that the pin or the disc lose material is smooth (in macroscopic scale) and always wear appears only in the contact area. Thus demonstrating a way that the wear depth would obey a specific function, the *Wear Depth Function*, for all the nodes that are in contact, the problem could be formulated in terms of sensitivity analysis and shape identification.

Taking into account the simple geometry of a *pin on disc* problem, which is a non-conformal symmetric contact problem, and considering the resulting pressure distribution, it can be shown that the wear depth obeys a parabolic law given by

$$h_i^H = c_1^H \left(x_i^H\right)^2 + c_2^H \tag{8}$$

[1] This assumption is valid only for cases not subjected to severe wear. More details are discussed in Section 8.

where c_1^H, c_2^H are the parameters of the above parabolic wear and more specifically c_2^H is the maximum wear depth. The term x_i^H denotes the x-coordinates of the contact nodes of body A and B, in two-dimensional problems. The above function corresponds only to the nodes that are in contact.

Depending on the design variables c_1^H and c_2^H, Eq. (8) takes the form of an almost straight line or an almost circular arc. Thus problems where either one or both bodies lose material (independently if it is the pin or the disc), can be formulated in this way. A more detailed discussion about the wear depth functions and their limitations is included later in the Discussion and Conclusions section of the present paper.

6. Solution algorithms

6.1. Incremental method

The common technique for simulating wear problems is the *Incremental Method*. The main drawback of the specific method is the computational time that increases dramatically when practical sliding distances or machining times are considered. The *Incremental Method* is used in the present work to compare and validate the results of the proposed *Optimization Method*. This method has been used successfully for simulating wear experiments (Põdra and Andersson, 1999a,b; Serre et al., 2001; Sfantos and Aliabadi, in press).

6.2. Optimization method

The proposed algorithm uses a *Shape Optimization* technique to calculate the final geometry and wear depth of two bodies that are in contact and slide over each other. In this way a final geometry and wear depth is initially assumed and using optimization techniques, the "actual" final geometry is obtained after the minimization of an error function, that is called the objective function. No incrementation of the sliding distance is needed and the final solution is normally achieved after few iterations. Here the BFGS update (Broyden, 1970; Fletcher, 1970; Goldfarb, 1970; Shanno, 1970) is used and is briefly described in the Appendix A.

The general algorithm is composed by two different optimization routines, as illustrated in Fig. 4; the contact (inner) and the wear (outer) optimization routines. The outer loop is the main wear optimization routine, that assumes a final worn geometry, and then checks if it is the actual final geometry by minimizing an objective function. The inner optimization routine is used to adjust the assumed final geometry in order to reduce the "artificial" error inserted in the evaluation of the main objective function, by assuming a final worn geometry, which is not fully in contact. The assumed final geometry must satisfy the following conditions:

(a) The assumed final worn geometries to be fully in contact. This states to the fact that the bearing surfaces wear out only when they come in contact. Thus an assumption of a final geometry that would not be fully in contact after imposing the specified normal load, would result to inaccurate estimation of the wear objective function.
(b) The assumed final geometry should produce a rather smooth pressure distribution without any singularities at the contact edges. This is trivial as in the case of a non-conformal problem, like the one that is formulated here, the pressure distribution always vanishes to zero at the contact edges, before and after wear.

Therefore the assumed final geometry at the beginning of the algorithm, and for every iteration of the wear optimization routine, must fulfill the above conditions, after the application of the specified external load. The main objective function that is used for the contact optimization routine is the distance between the edge nodes of the assumed final geometries of the two bodies.

$$F(\mathbf{Z}_c^k) = \left| \mathbf{x}_{\text{edge}}^A + \mathbf{u}_{\text{edge}}^A - \mathbf{x}_{\text{edge}}^B - \mathbf{u}_{\text{edge}}^B \right| \tag{9}$$

where $\mathbf{x}_{\text{edge}}^H$ is the position vector of the edges' nodes of the assumed final geometries and $\mathbf{u}_{\text{edge}}^H$ is the corresponding displacement vector after the application of the specified load, for each body $H = \{A, B\}$. The term

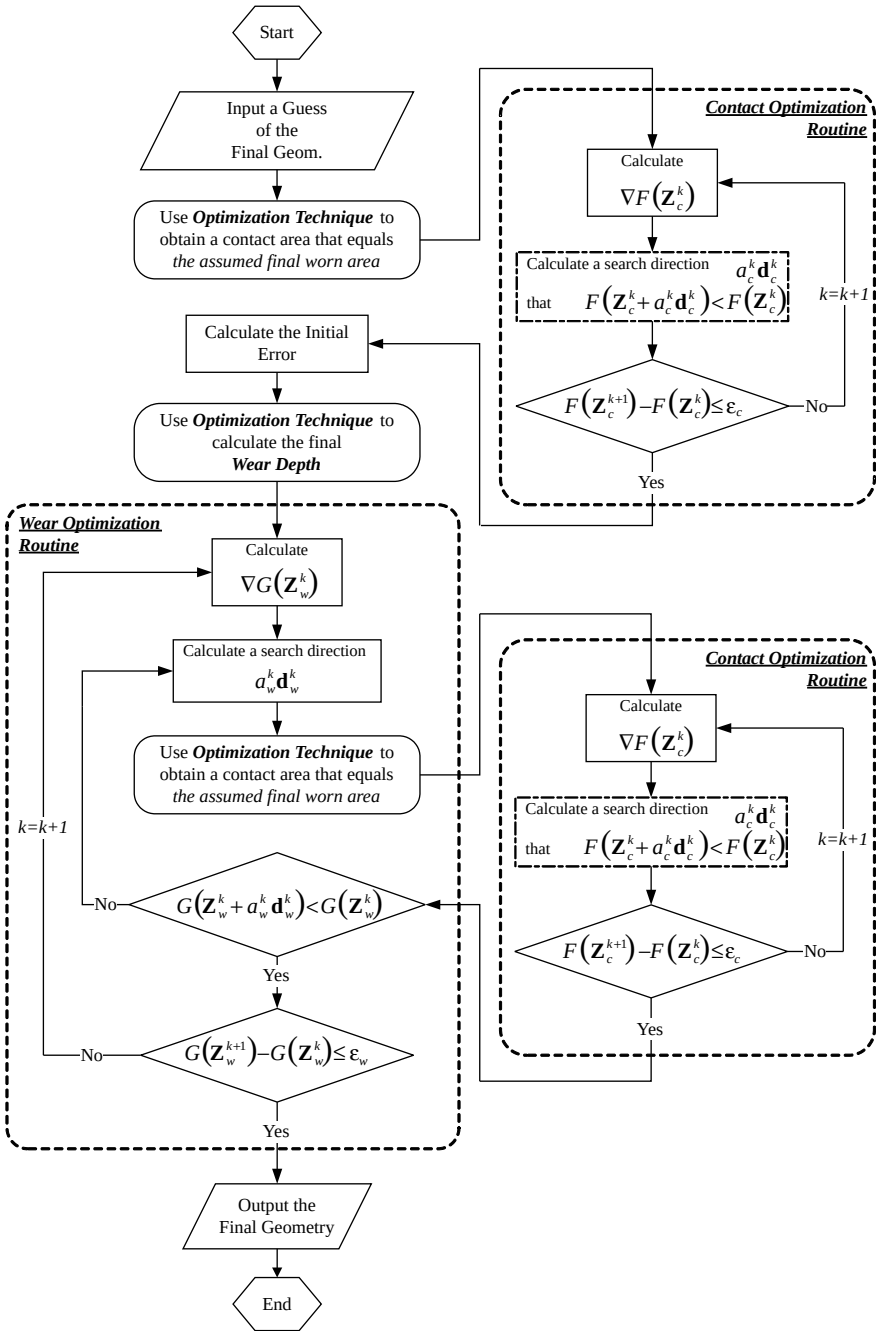

Fig. 4. Basic algorithm of the proposed *Optimization Method*.

$\mathbf{Z}_c^k$ denotes the design variable, where in the case of the inner loop is the constant c_1^H in the wear depth function (8).

Fig. 5 illustrates the proposed BEM and the internal sub-program used for the calculation of a search direction $a_c^k\mathbf{d}_c^k$ that satisfies the inequality $F(\mathbf{Z}_c^k + a_c^k\mathbf{d}_c^k) < F(\mathbf{Z}_c^k)$ (see Appendix A).

Since the assumed initial geometry satisfies all the above conditions the main wear optimization routine starts (outer loop). The objective function $G(\mathbf{Z}_w^k)$ that is used here is given by

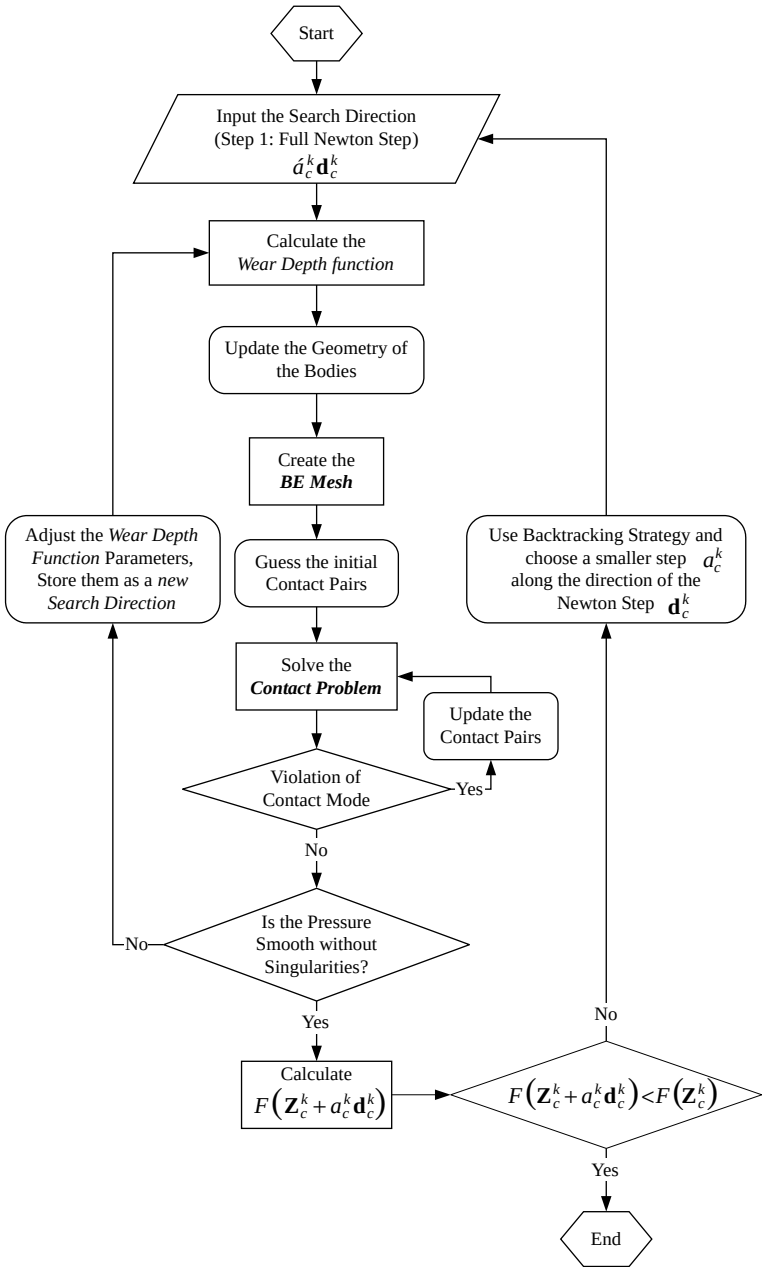

Fig. 5. Internal sub-program for the determination of the Contact optimization error function.

$$G\left(\mathbf{Z}_{\mathrm{w}}^k\right) = \frac{\sum_{i=1}^{M_{\mathrm{c}}} \left|\mathbf{x}_i^0 - \left(\mathbf{x}_i^{\mathrm{f}} - \mathbf{h}_i\right)\right|^A}{M_{\mathrm{c}}} + \frac{\sum_{i=1}^{M_{\mathrm{c}}} \left|\mathbf{x}_i^0 - \left(\mathbf{x}_i^{\mathrm{f}} + \mathbf{h}_i\right)\right|^B}{M_{\mathrm{c}}} \tag{10}$$

where $\mathbf{x}_i^0$ and $\mathbf{x}_i^{\mathrm{f}}$ correspond to the initial and assumed final positions, respectively, of every node $i = 1$, M_{c}, of the potential contact area for both bodies A and B, and $\mathbf{h}_i$ is the wear depth vector corresponding to the specific node i of the potential contact area. The wear vector is taken to coincide with the pressure vector; that is normal to the bearing surface of the body in contact. Eq. (10) demonstrates that the assumed final geometry is the actual final geometry when the mean difference of the initial geometry of the bodies, compared to the assumed final geometry plus the wear depth, becomes zero. The term $\mathbf{Z}_{\mathrm{w}}^k$ denotes the design variable, where in the case of the outer loop is the constant c_2^H (wear depth) in the wear depth function (8).

The main wear optimization routine starts by calculating the derivatives of the objective function in terms of every design variable using the forward scheme of the Finite Difference method, Eq. (17) in the Appendix A. Taking into consideration the derivatives of the objective function (10) with respect to every design variable, a search direction is chosen. Then the contact optimization routine is called again in order to obtain a search direction that decreases the objective function (9) in order the assumed worn geometry to be also a contact geometry. This procedure is followed until the objective function is sufficiently decreased comparing it with the initial error. When it is sufficiently decreased then the error of the current step is compared with the previous step. If convergence is achieved to some specified tolerance then the algorithm comes out of the wear optimization loop and the final geometry with the final wear depth is obtained. Otherwise new derivatives are calculated, a new search direction is obtained and the algorithm continues.

7. Numerical examples

In this section the proposed formulation is applied to one body and two bodies wear simulation. The proposed method is compared with a boundary element incremental method (Sfantos and Aliabadi, in press). The incremental method used here, has already been tested for each validity against analytical solutions and other reported numerical solutions using the FEM (Põdra and Andersson, 1999a). For more details the authors are referred to Sfantos and Aliabadi (in press). In the following numerical examples, the disc diameter is assumed very large compared to the pin diameter and the position of the pin is far from the center of revolution of the disc. Consequently as the disc rotates, the difference of the travelled distance between points on the bearing surface of the pin can be neglected and thus all points on the pin, either in contact or not, is assumed to travel exactly the same distance (Põdra and Andersson, 1999a).

7.1. One body wear formulation

In order to validate the proposed *Optimization Method* for the solution of wear problems, the classic pin-on-disk wear experiment was formulated as a first step. Table 3 presents the parameters used for the specific problem, while Fig. 6 illustrates a schematic representation of the physical problem and its boundary element model. In this example each body was modelled using 50 quadratic elements in total, whereas 49 nodes (24 elements) were used to compose the potential contact area. For the proposed method an initial guess of the maximum wear depth was made at $h^A_{\max} = 5 \times 10^{-4}$ mm. The initial pressure distribution calculated by the BEM is illustrated in Fig. 7. In the same figure the initial pressure calculated analytically by Hertzian theory (Hertz, 1882) and the pressure after sliding 0.5 m calculated by the proposed method, are also illustrated for comparison. It is obvious that the initial pressure, calculated by the BEM is in good agreement with the Hertzian solution. The pressure distribution of the worn pin is flattened compared to the initial; as it was expected this is due to the material loss. Fig. 8 illustrates the deviation of the wear objective function $G(\mathbf{Z}^k_w)$ and the maximum wear depth $h^A_{\max}$ of the pin in respect to the number of iterations needed to achieve convergence. The results obtained by the proposed method versus the *Incremental Method* in terms of the final geometry of the worn pin are presented in Fig. 9. For illustration reasons the worn geometries of the pin, obtained by different increments using the incremental method, are illustrated in Fig. 9 by pointed lines, representing the position of each node composing the worn area. It can be seen that the "artificial" roughness introduced by the incremental method is absent in the case of the proposed method due to the use of the wear depth

Table 3
Parameters for the one-body-wear problem

Wear coefficient	$k^A = 1.33 \times 10^{-13}\ \mathrm{Pa}^{-1}$
Total sliding distance	$S = 0.5$ m
Normal load	$P = 4.63$ N/mm
Poisson ratio	$v_A = v_B = 0.3$
Radius of the pin	$R^A = 10 \times 10^{-3}$ m
Elastic moduli	$E^A = E^B = 70$ GPa
Initial guess	$h^A_{\max} = 5 \times 10^{-4}$ mm, $c^A_1 = 0.015$

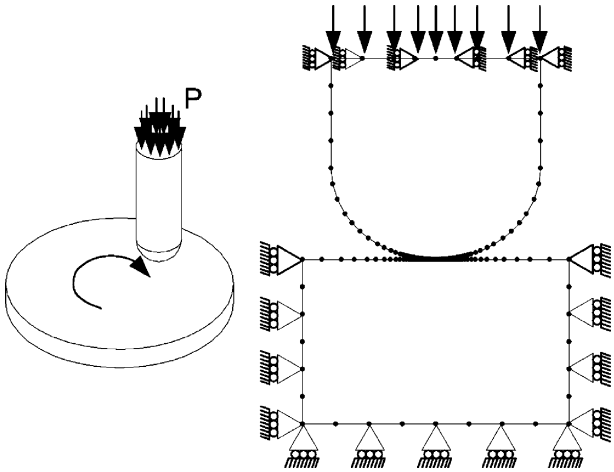

Fig. 6. A schematic representation of the pin-on-disk wear problem formulated in the present paper and its boundary element model.

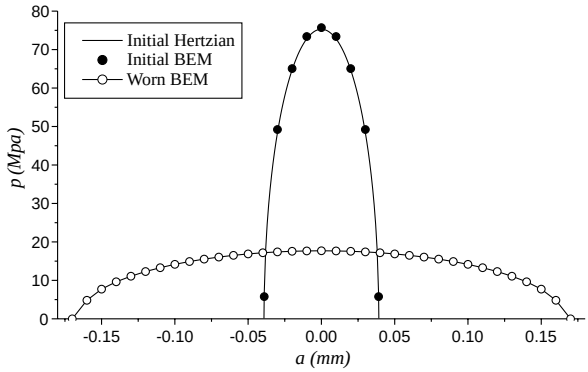

Fig. 7. Initial pressure distribution (by the BEM and Hertz theory) and worn pressure distribution after sliding 0.5 m; a, width of contact area and p, pressure.

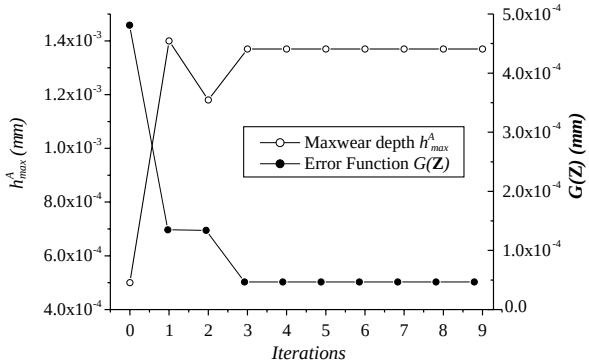

Fig. 8. Wear depth and error function using the *Optimization Method* for the one-body-wear problem.

function. The maximum wear depth calculated by the incremental method, for the specific problem, was 1.372×10^{-3} mm, while by the optimization method was 1.37×10^{-3} mm; the difference is less than 0.15%.

As it can be seen from Fig. 8 only four iterations were required for the proposed method to achieve the final maximum wear depth and geometry of the pin, while in the incremental method (with 2.5 mm sliding incre-

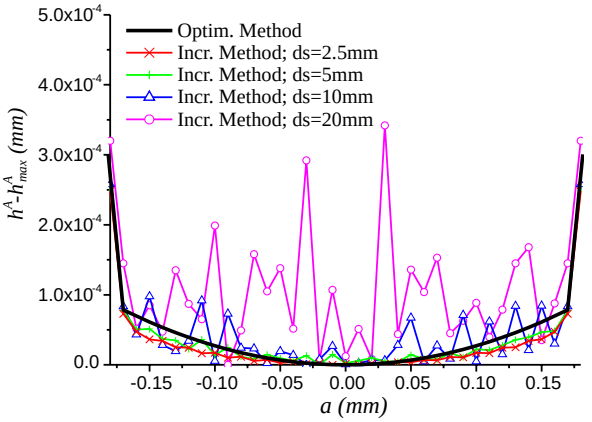

Fig. 9. Final geometry of the pin by the incremental and the proposed method; a, width of contact area.

ments, for a total distance of 500 mm), 200 iterations were required. Using a Pentium PC 2.2 GHz processor the proposed method was about eight times faster than the *Incremental Method*. The reduction in time using the *Optimization Method* is considered to be significant. In practical case problems, where the sliding distances are large, using small sliding increments to achieve converged smooth final geometry and maximum wear depth, the *Incremental Method* might need thousands of iterations. On the other hand the proposed method after an approximate initial guess would need only some iterations. This is because the BFGS algorithm converges fast when the objective function is close to a quadratic function and in addition when the assumed solution is close to the final solution. By using the full Newton step for the scalar multiplier, as described previously, quadratic convergence is achieved (Fletcher, 1980; Bazaraa et al., 1993).

To validate the above conclusion a larger scale problem was modelled in order to compare the CPU time between the two methods. In this example each body, Fig. 6, was modelled using 82 quadratic elements, whereas 97 nodes (48 elements) were used to compose the potential contact area. The same material parameters were used; Table 3. In the case of the *Incremental Method* three different increment sizes were used for the aim of checking which increment produces acceptable results requiring less CPU time. The total sliding simulated distance was $S = 13.0$ m. In order to compare the maximum wear depth and the CPU time with respect to the sliding distance calculated by the *Incremental Method* and the *Optimization Method,* the following method was used. For certain sliding distances an initial guess with >50% error (compared to the actual max. wear depth given by the incremental method) was used as input data for the *Optimization Method.* Fig. 10 illustrates the maximum wear depth with respect to the sliding distance obtained by both methods.

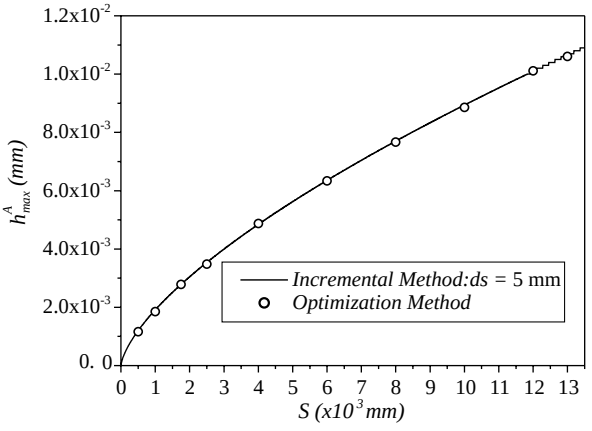

Fig. 10. Maximum wear depth with respect to the sliding distance.

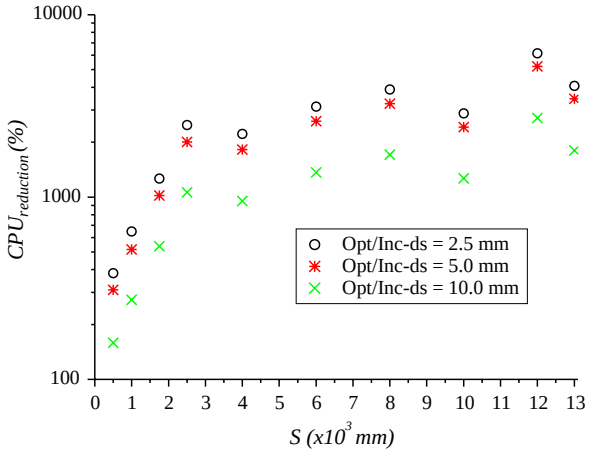

Fig. 11. CPU time reduction with respect to the sliding distance by using the *Optimization Method* instead of the *Incremental*, for various sliding increments.

It must be noted that the calculated maximum wear depth, by the *Optimization Method*, differs less than 1% compared to the corresponding values using the *Incremental Method*. Fig. 11 illustrates the relative reduction in CPU time by using the proposed *Optimization Method,* with respect to the time the *Incremental Method* spent to simulate the same problem for various sliding increments. The ordinate of the graph in Fig. 11 is calculated as follows:

$$\mathrm{CPU}_{\mathrm{reduction}} = \frac{\mathrm{CPU}_{\mathrm{Incr}}}{\mathrm{CPU}_{\mathrm{Opt}}} \cdot 100\%$$

It is shown that as the sliding distance increases the reduction of the CPU time using the proposed method is significant.

7.2. Two bodies wear formulation

In case both bodies wear out in comparable time, the problem becomes more complicated as both bearing surfaces change with respect to the sliding distance. Using the proposed method, the main difference comparing with the one-body wear formulation, is that two wear depth functions must be used, i.e. Eq. (8), where the constant term (max. wear depth) of each function is given by[2]

$$\begin{aligned} c_2^A &= h_{\max}^A \\ c_2^B &= h_{\max}^A \frac{k^B}{k^A} \end{aligned} \tag{11}$$

Thus considering the basic algorithm of the proposed method, Fig. 4, the outer wear optimization routine is used to evaluate the wear depth $h_{\max}^A$ that minimizes the specific objective function $G(\mathbf{Z}_w)$, Eq. (10). The inner contact optimization algorithm evaluates the parameters of the two wear depth functions, Eq. (8), given as c_1^A and c_1^B, in order the objective function $F(\mathbf{Z}_c)$, Eq. (9) to be minimized.

The parameters used for the specific problem are presented in Table 4. Fig. 12 illustrates the deviation of the wear objective function $G(\mathbf{Z})$ and the maximum wear depth $h_{\max}^A$ and $h_{\max}^B$ of the pin and the disc respectively, in respect to the number of iterations required to achieve convergence. The maximum wear depth of each body is exactly the same as both bodies had the same wear coefficient as Table 4 illustrates. Fig. 13 illustrates the final geometry at each optimization step, up to the 3rd, where the final geometry was achieved. The resulting

[2] For simplification, it is assumed that all contact node pairs, of the potential contact-worn areas of both bodies, slide exactly the same distance.

Table 4
Parameters for two-bodies-wear problem

Wear coefficient	$k^A = 0.665 \times 10^{-13}$ Pa^{-1}, $k^B = 0.665 \times 10^{-13}$ Pa^{-1}
Total sliding distance	$S = 0.5$ m
Normal load	$P = 4.63$ N/mm
Poisson ratio	$v_A = v_B = 0.3$
Radius of the pin	$R^A = 10 \times 10^{-3}$ m
Elastic moduli	$E^A = E^B = 70$ GPa
Initial guess	$h^A_{\max} = 5 \times 10^{-4}$ mm, $c^A_1 = 0.022$, $c^B_1 = 0.022$

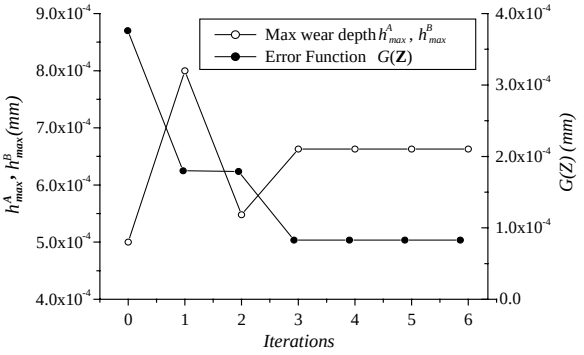

Fig. 12. Wear depth and error function using the *Optimization Method* for two-bodies-wear problem.

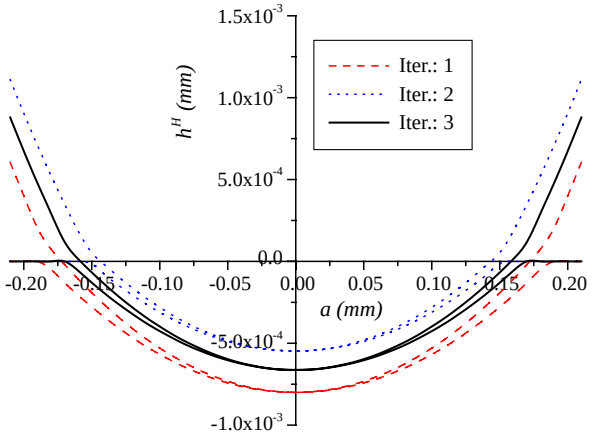

Fig. 13. Predicted final geometries of the pin (upper line) and the disc (lower line) in respect to the iterative step of the *Optimization Method*; *a*, width of contact area.

geometries obtained by the proposed method versus the *Incremental Method* are illustrated in Fig. 14. It is obvious that the resulting final worn geometry and the maximum wear depth calculated by the proposed method and the incremental are in good agreement. The assumption that all contact node pairs slide the same distance was made just for simplification and comparison with the incremental method (Sfantos and Aliabadi, in press), and it does not provide any limitation in the above formulation. Without great effort, the total sliding distance that a specific node would have travelled, evaluated by the kinematics of the tribosystem, should be used in the modified wear law, Eq. (4), every time it is used to evaluate the wear depth for the specific node, during the optimization process.

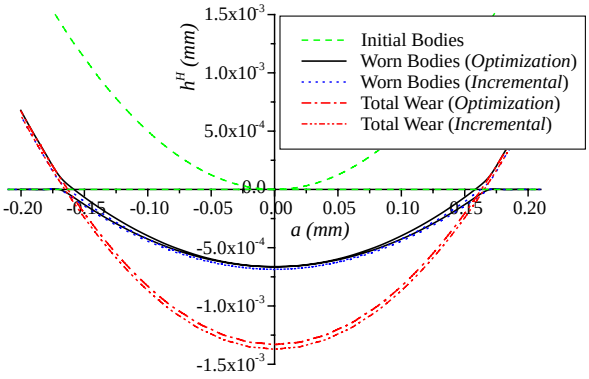

Fig. 14. *Optimization Method* versus *Incremental Method,* when both bodies wear; *a*, width of contact area.

8. Discussion and conclusions

In the present paper a Boundary Element methodology for modelling wear using an optimization technique was presented. The following conclusions are derived based on the results presented:

(i) The advantage of the proposed *Optimization Method*, is that it solves a wear problem for a specified service period, using only few iterations, in contrast to many iterations required by the classic *Incremental Method*. The total CPU time required to achieve the final solution is reduced substantially as the sliding distance is increased.
(ii) The resulting final geometry and pressure distribution using the proposed method are always smooth. This is in contrast to the *Incremental Method* whose the sliding increment must be very small compared to the total sliding distance to achieve a smooth solution.
(iii) The proposed method does not require any *trial and error* procedure to select the appropriate sliding increment.
(iv) Generally, the computational effort remains low as only *boundary* modelling is required. This is a great advantage considering the wear simulation problems, where the geometry is updated after every step.

From the concluding remarks, it is obvious that the proposed formulation provides sufficient advantages over the classic incremental method. However there are certain limitations that must be addressed and certain problems requiring special attention. These limitations are discussed next.

The wear depth function used in the proposed formulation requires special attention considering each tribosystem. In the present paper a simple parabolic function was used, just to demonstrate the proposed method. However different kinds of functions can be used with respect to the wear problem. For example in the case of a general non-conformal problem, the wear depth function can be a polynomial of the gap function of the undeformed bodies. Thus in this way the history of the initial unworn geometries is carried out throughout the solution. In the opposite case of a conformal contact, the wear depth function can be a polynomial of the initial pressure distribution. In cases involving more complicated geometries, as asymmetric contacts and multi-contacts, more than one wear depth functions can be used for different areas of the potential worn surface.

The main disadvantage of the proposed method is that it is restricted to problems requiring only the final solution. Wear problems in which the evolution of wear is of interest, the proposed formulation can not provide any information except from the final geometry and wear depth. These type of problems can be solved only by the incremental method, which can simulates the wear evolution. Another disadvantage of the proposed formulation is that it is restricted to wear problems under static load. In cases of variable loading the optimization method, in the present form, can not provide any solution, as its basic concept requires all the external boundary conditions to be constant. Finally for tribosystems subjected to severe wear, e.g. in the case of a pin-on-disk where the spherical end of the pin wears out completely, the proposed formulation

can not be used as the pressure distribution at that time does not provide the details the modified wear law needs to evaluate the initial geometry by solving inversely.

Throughout the analysis, it was demonstrated that the proposed formulation provides accurate results, sufficiently fast. Thus the proposed method seems to be a promising tool for simulating wear in cases where only the final geometry and maximum wear depth are required, during the designing stage of a mechanical component. However more research is required to address the limitations and the restrictions of the presented method.

Appendix A

The BFGS update (Broyden, 1970; Fletcher, 1970; Goldfarb, 1970; Shanno, 1970) for the $\mathbf{H}^k$ matrix, is given by

$$\mathbf{H}^{k+1} = \mathbf{H}^k - \left[\frac{\mathbf{H}^k\mathbf{q}^k(\mathbf{p}^k)^{\mathrm{T}} + \mathbf{p}^k(\mathbf{q}^k)^{\mathrm{T}}\mathbf{H}^k}{(\mathbf{p}^k)^{\mathrm{T}}\mathbf{q}^k}\right] + \left[\mathbf{I} + \frac{(\mathbf{q}^k)^{\mathrm{T}}\mathbf{H}^k\mathbf{q}^k}{(\mathbf{p}^k)^{\mathrm{T}}\mathbf{q}^k}\right]\left[\frac{\mathbf{p}^k(\mathbf{p}^k)^{\mathrm{T}}}{(\mathbf{p}^k)^{\mathrm{T}}\mathbf{q}^k}\right] \tag{12}$$

where $\mathbf{I}$ is the identity matrix, $()^{\mathrm{T}}$ denotes the transpose matrix, and $\mathbf{q}^k$, $\mathbf{p}^k$ are given as

$$\begin{aligned}\mathbf{p}^k &= \mathbf{Z}^{k+1} - \mathbf{Z}^k \\ \mathbf{q}^k &= \nabla F(\mathbf{Z}^{k+1}) - \nabla F(\mathbf{Z}^k)\end{aligned} \tag{13}$$

The $\mathbf{H}^k$ matrix is a series of matrices, beginning with the identity matrix $\mathbf{I}$ and ending with an approximation to the inverse Hessian matrix $\mathbf{H}^{-1}$, a positive definite symmetric matrix of the second partial derivatives of the objective function in terms of the design variables.

The line search direction is given by the following equation (Bazaraa et al., 1993):

$$\mathbf{Z}^{k+1} = \mathbf{Z}^k + a^k\mathbf{d}^k \tag{14}$$

where $\mathbf{Z}^{k+1}$ is the column vector of the updated design variables, $\mathbf{d}^k$ is the computed search direction where the function $F(\mathbf{Z})$ is decreased and a^k is a scalar multiplier such that the function $F(\mathbf{Z}^k + a^k\mathbf{d}^k)$ is minimized. The computed search direction is given as

$$\mathbf{d}^k = -\mathbf{H}^k\nabla F(\mathbf{Z}^k) \tag{15}$$

The above process is repeated until the objective function converges to some predefined tolerance, ε, that is

$$F(\mathbf{Z}^{k+1}) - F(\mathbf{Z}^k) \leqslant \varepsilon \tag{16}$$

The derivatives of the objective function, in Eqs. (13) and (15), can be calculated using the forward scheme of the Finite Difference method, in respect to every design variable, given by

$$\nabla F(\zeta_i) = \frac{F(\zeta_i + \delta_i) - F(\zeta_i)}{\delta_i} \tag{17}$$

where δ_i is the step corresponding to every design variable ζ_i for $i = 1, m$.

The procedure starts with a positive definite and symmetric matrix, which is usually the identity matrix, and then the approximations of the Hessian matrix $\mathbf{H}^k$ are build in a way that they remain positive definite and symmetric. In the case that the solution is still far from the optimum, this way of updating the matrix guarantees that the design variables will always move in a downhill direction, where the objective function is decreasing. When the design variables are close to the optimum solution, then the updating formula approaches the true Hessian matrix and the quadratic convergence of Newton's method is achieved (Bazaraa et al., 1993).

References

Aliabadi, M.H., 2002. The Boundary Element Method. Applications in Solids and Structures, vol. 2. Wiley, London.

Aliabadi, M.H., Mellings, S.C., 1997. Boundary Element Formulations for Sensitivity Analysis and Crack Identification. Boundary Integral Formulation for Inverse Analysis. Computational Mechanics Publications, Southampton.

Archard, J.F., 1953. Contact and rubbing of flat surfaces. J. Appl. Phys. 24, 981–988.
Bazaraa, M.S., Sherali, H.D., Shetty, C.M., 1993. Nonlinear Programming, Theory and Algorithms, second ed. Wiley, New York.
Broyden, C.G., 1970. The convergence of a class of double-rank minimization algorithms. J. Inst. Math. Appl. 6, 76–90.
Fletcher, R., 1970. A new approach to variable metric algorithms. Computer Journal 13, 317–322.
Fletcher, R., 1980. Practical Methods of OptimizationUnconstrained Optimization, vol. 1. Wiley.
Goldfarb, D., 1970. A family of variable metric updates derived by variational means. Math. Comput. 24, 23–26.
Hertz, H., 1882. Über die Berührung fester elastischer Körper. J. Reine Angew. Math. 92, 156–171 (On the contact of elastic solids).
Holm, R., 1946. Electric Contacts. Gebers, Stockholm.
Johnson, K.L., 2001. Contact Mechanics. Cambridge University Press, Cambridge.
Lim, S.C., Ashby, M.F., 1987. Wear-mechanism maps. Acta Metall. 35 (1), 1–24.
MacGinley, T., Monaghan, J., 2001. Modelling the orthogonal machining process using coated cemented carbide cutting tools. J. Mater. Proc. Technol. 118, 293–300.
Man, K., Aliabadi, M.H., Rooke, D.P., 1993a. BEM frictional contact analysis: an incremental loading technique. Comput. Struct. 47, 93–905.
Man, K., Aliabadi, M.H., Rooke, D.P., 1993b. BEM frictional contact analysis: modelling considerations. Eng. Anal. Bound. Elem. 11, 77–85.
Martinez, M.J., Aliabadi, M.H., Power, H., 1998. Bone remodelling using sensitivity analysis. J. Biomech. 31, 1059–1062.
Maxian, T.A., Brown, T.D., Pedersen, D.R., Callaghan, J.J., 1996a. A sliding-distance-coupled finite element formulation for polyethylene wear in total hip arthroplasty. J. Biomech. 29, 687–692.
Maxian, T.A., Brown, T.D., Pedersen, D.R., Callaghan, J.J., 1996b. 3-Dimensional sliding/contact computational simulation of total hip wear. Clin. Orthopaed. Relat. Res. 333, 41–50.
Mellings, S.C., Aliabadi, M.H., 1995. Flaw identification using the boundary element method. Int. J. Numer. Meth. Eng. 38, 399–419.
Peigney, M., 2004. Simulating wear under cyclic loading by a minimization approach. Int. J. Solids Struct. 41, 6783–6799.
Põdra, P., Andersson, S., 1999a. Simulating sliding wear with finite element method. Tribol. Int. 32, 71–81.
Põdra, P., Andersson, S., 1999b. Finite element analysis wear simulation of a conical spinning contact considering surface topography. Wear 224, 13–21.
Rabinowicz, E., 1995. Friction and Wear of Materials, second ed. Wiley, New York.
Serre, I., Bonnet, M., Pradeilles-Duval, R.-M., 2001. Modelling an abrasive wear experiment by the boundary element method. CR Acad. Sci. Paris 329 (Série II b), 803–808.
Sfantos, G.K., Aliabadi, M.H., in press. Wear simulation using an incremental sliding boundary element method. Wear.
Shanno, D.F., 1970. Conditioning of quasi-Newton methods for function minimization. Math. Comput. 24, 647–656.
Wu, J.S.-S., Hung, J.-P., Shu, C.-S., Chen, J.-H., 2003. The computer simulation of wear behaviour appearing in total hip prosthesis. Comput. Meth. Prog. Biomed. 70, 81–91.
Yen, Y.-C., Söhner, J., Lilly, B., Altan, T., 2004. Estimation of tool wear in orthogonal cutting using the finite element analysis. J. Mater. Proc. Technol. 146, 82–91.